

Quantifying the Building Blocks of Igneous Rocks: Are Clustered Crystal Frameworks the Foundation?

DOUGAL A. JERRAM^{1*}, MICHAEL J. CHEADLE² AND ANTHONY R. PHILPOTTS³

¹DEPARTMENT OF GEOLOGICAL SCIENCES, UNIVERSITY OF DURHAM, SCIENCE LABORATORIES, SOUTH ROAD, DURHAM DH1 3LE, UK

²DEPARTMENT OF GEOLOGY AND GEOPHYSICS, UNIVERSITY OF WYOMING, LARAMIE, WY 82071-3006, USA

³DEPARTMENT OF GEOLOGY AND GEOPHYSICS, UNIVERSITY OF CONNECTICUT, STORRS, CT 06269, USA

RECEIVED JUNE 5, 2002; ACCEPTED MAY 12, 2003

Most phenocryst populations in volcanic rocks, and those preserved in shallow-level igneous intrusions, are clustered (variously referred to as clots, clumps or glomerocrysts). These clusters of crystals are the building blocks that accumulate to form the high-porosity, touching crystal frameworks from which igneous cumulates form. Examination of touching crystal frameworks in olivine- (komatiite cumulates and experimental charges) and plagioclase-dominant crystal populations (Holyoke flood basalt, Connecticut, USA) reveal complex, high-porosity, clustered crystal arrangements. Olivine touching frameworks in komatiite flows are interpreted to form in hundreds of days. Plagioclase frameworks are calculated to have formed in less than 17 years for a crystal growth rate of 1×10^{-10} mm/s to less than 3 years for a growth rate of 5×10^{-10} mm/s based on crystal size distributions. The origin of crystal clusters is likely to involve either (or a combination of) heterogeneous nucleation, remobilization of cumulate mushes or crystals sticking together during settling and/or flow. The spatial distribution pattern of clustered crystal frameworks from both natural and experimental examples constrains fields on spatial packing diagrams that allow the identification of touching and non-touching crystal populations, and further improve our understanding of crystal packing arrangements and cluster size distributions.

KEY WORDS: cumulates; CSD; komatiite; basalt; spatial packing; textural analysis

INTRODUCTION

Most phenocryst populations in volcanic rocks are not made up solely of individual crystals but contain mixtures of both individual crystals and clusters of touching crystals. These clusters are also variously referred to as clumps, clots or glomerocrysts (Garcia & Jacobson, 1979; Schwingdinger & Anderson, 1989; Silva *et al.*, 1997; Jerram & Cheadle, 2000) and are important because they are the basic unit 'building blocks' from which many igneous textures develop. Figure 1 shows the markedly different textures produced when frameworks of crystals are produced using clustered-clumped or individual-single phenocrysts as building blocks. If a framework is produced from a mixed population of irregular-shaped clusters or clumps of crystals, the resulting framework will contain a high melt porosity and be loosely packed (Fig. 1a). Conversely, frameworks that are constructed from individual crystals will have a more tightly packed arrangement of crystals with a lower melt porosity (Fig. 1b). As the modal abundance of the framework-building phase is reduced a more intricate clustered or chained network is required to remain touching in three dimensions (Fig. 1c). A detailed understanding of the packing structure of crystals, a knowledge of whether cumulate phases produce touching frameworks in three dimensions, and a quantification of the units (building blocks) that produce cumulates are all fundamental

*Corresponding author. Telephone: ++44 (0)191 334 2281. Fax: ++44 (0)191 334 2301. E-mail: D.A.Jerram@dur.ac.uk

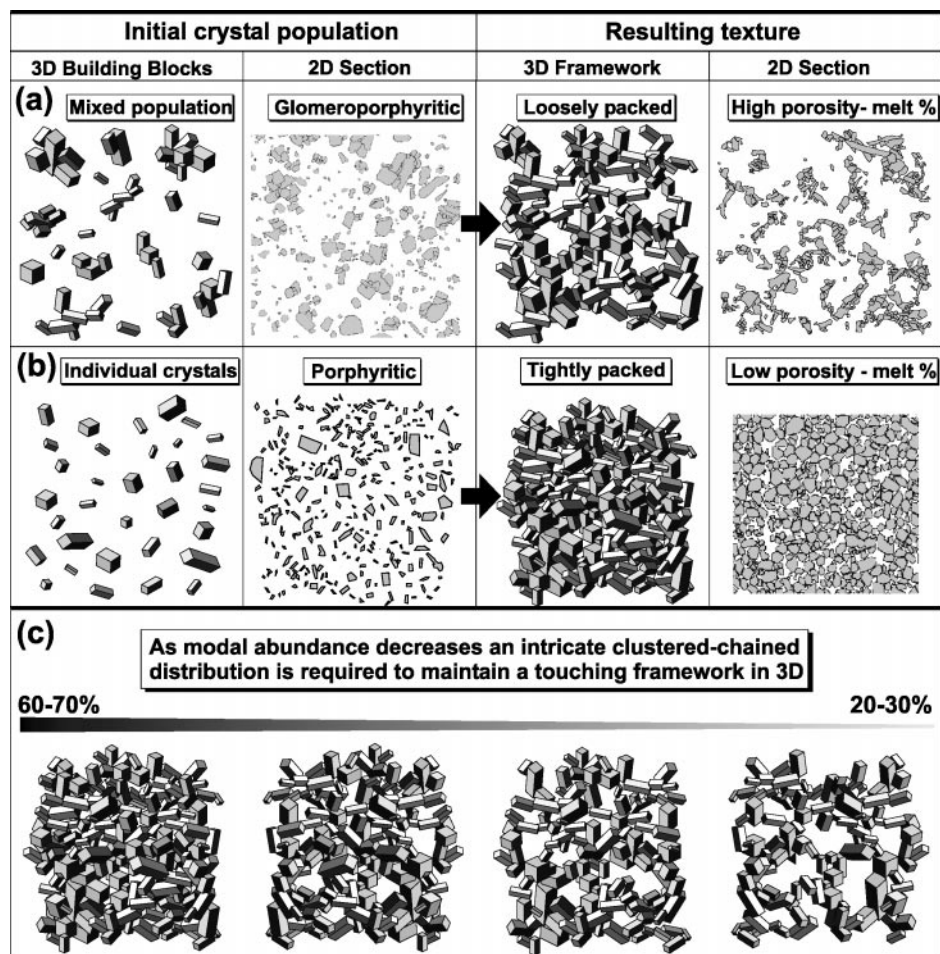


Fig. 1. The development of crystal frameworks using phenocryst populations as initial 'building blocks'. (a) The initial 'building blocks' consist of a mixed population of clustered (clumped) and individual crystals. (b) The initial 'building blocks' consist of a population of individual crystals. (c) Touching crystals show markedly different spatial packing arrangements in order to maintain their frameworks at different modal abundance.

observations required for deciphering how igneous cumulates form.

The generation of igneous cumulates and igneous layering remains the focus of much debate, with many conflicting models, e.g. crystal settling, *in situ* growth, gravity currents, and redistribution of phases during compaction (e.g. Eales & Cawthorn, 1996; Emeleus *et al.*, 1996; Boudreau & McBirney, 1997), despite years of study. However, a major question still remains unanswered: are the initial accumulations of crystals in layered igneous rocks formed from clustered crystal populations or from individual crystals or both? Magmas are commonly laced with high population densities of nuclei, super-nuclei, and crystallites or clusters that together set the initial characteristics of the crystal population (Marsh, 1998), a system that favours heterogeneous nucleation. Further evolution of the crystal population occurs through sustained

heterogeneous nucleation and annealing (Marsh, 1998). Indeed, the propensity for heterogeneous nucleation vs homogeneous nucleation in magmas (e.g. Burkhard, 2002) means that clusters of crystals are likely to be common in a crystallizing magma. If crystal populations have the tendency to be clustered, what are the implications for how such crystal frameworks develop under post-accumulation compaction and overgrowth? One way to address this issue is to look at examples of crystal accumulation where little or no textural modification or equilibration has occurred. By quantifying such textures we may firstly gain insight into how the initial clustered textures develop and secondly be able to understand how they are modified during post-cumulus processes to produce the actual textures we see in more slowly cooled igneous rocks.

Crystal populations that form in a melt, if allowed to continue crystallizing, develop into a touching crystal

framework, a crystal mush (e.g. Marsh, 1996, 2002), which with further crystallization and possible post-cumulus equilibration eventually produces the final igneous texture. A range of textures will be produced during the growth history of the crystal population; the challenge is to find examples of those textures that have been arrested or frozen-in, before solidification or crystallization has gone to completion (e.g. a lava flow, dyke or sill chilled margin that preserves the crystal population early in its development). Once such examples have been found, the next task is to characterize and quantify textural parameters (e.g. crystal sizes and packing arrangements) to help understand the early stages of texture development. However, the recognition of clustered touching crystal frameworks is difficult. We require some means to be certain that structures with low crystal proportions, representing high-porosity frameworks, are actually touching in three dimensions and do not just represent crystals suspended in a melt that quenched in the texture. The existence of very high-porosity (75%) frameworks of micro-crystals has been demonstrated in basalt melting experiments (e.g. Philpotts & Carroll, 1996; Philpotts *et al.*, 1998); these results reveal the possible extent of clustering within magmatic systems at very low crystal proportions. The ability to image and model textures in three dimensions (e.g. Carlson *et al.*, 1999; Philpotts *et al.*, 1999; Jerram, 2001), along with two-dimensional (2D) measurements from sections through touching crystal frameworks (e.g. komatiite cumulates), can be used to test and refine textural analysis techniques (e.g. Bryon *et al.*, 1995; Cooper & Hunter, 1995; Jerram *et al.*, 1996; Jerram & Cheadle, 2000) with a view to providing an approach for identifying touching crystal frameworks from less well-constrained textures.

In this paper we examine touching crystal frameworks in both olivine- and plagioclase-dominant crystal populations from lava flows of differing thickness. Olivine-touching frameworks in examples of komatiite lava flows from the Abitibi greenstone belt (Canada), Kambalda (Australia), Vammala (western Finland), and the Belingwe greenstone belt (Zimbabwe) are quantified using textural analysis techniques describing spatial packing (e.g. Jerram *et al.*, 1996). These are igneous bodies that are a few metres to tens of metres thick. A detailed suite from a single flow (Joe's Flow komatiite) in the Belingwe greenstone belt, Zimbabwe, is then examined further using dihedral angle measurements, mineral composition data, and crystal size distributions (CSDs), to constrain the origin of clustering in crystal populations and the growth rates of the individual crystals. Plagioclase touching and non-touching frameworks, revealed by melting experiments on the 200 m thick Holyoke flood basalt, Connecticut,

USA (Philpotts & Carroll, 1996; Philpotts *et al.*, 1998), are quantified to further constrain spatial packing arrangements and formation of clustered crystal frameworks. Crystal growth rates are also constrained by CSD measurements. Finally, we use the examples of clustered and non-clustered crystal frameworks to populate a plot of spatial distribution pattern vs porosity (% melt) (Jerram *et al.*, 1996). This defines areas on the plot that can be used to determine the spatial characteristics of a rock texture (is the crystal packing clustered, random or ordered?), and whether textures form a touching framework or not.

METHODS OF TEXTURAL ANALYSIS

Recent advances in petrographic studies have been greatly enhanced by image analysis programs developed mainly within the biological sciences. Image analysis software is designed to recognize and analyse objects identified in digital images on the computer, often working with bitmap digital images of the sample to be studied. Such software can be used to provide shape, size and positional data on the objects of interest. The data obtained from such analyses can then be used to quantify important information about, for example, size distributions or spatial patterns within and between samples of interest.

Sample preparation and image analysis

To quantify objects within a rock texture we must first input the textural information into the image analysis software. This process is non-trivial as the objects of interest in rock textures (grains or crystals) are often fractured, touching and have differing optical properties, which make them difficult to be automatically identified by the computer. The approach taken in the present study is summarized by a flow diagram in Fig. 2, as used in previous studies (e.g. Jerram *et al.*, 1996; Jerram & Cheadle, 2000; Mock *et al.*, 2003). Individual crystals are identified, with the aid of a microscope, and outlined. This process can be performed on high-resolution prints of the texture with use of an overlay, or directly on digital images within computer graphics packages. This process allows the user to correctly identify the crystals within the sample and to edit the texture into a simple bitmap format for the image analysis software. The bitmap image is then opened into the image analysis software, the image scale is set, and the objects (in this case crystals) in the image are then analysed for their *xy* grain centre co-ordinates and the orientation and lengths of their long and short axes. This textural information is then used to quantify the crystal spatial distribution pattern and crystal size distribution analyses as described below.

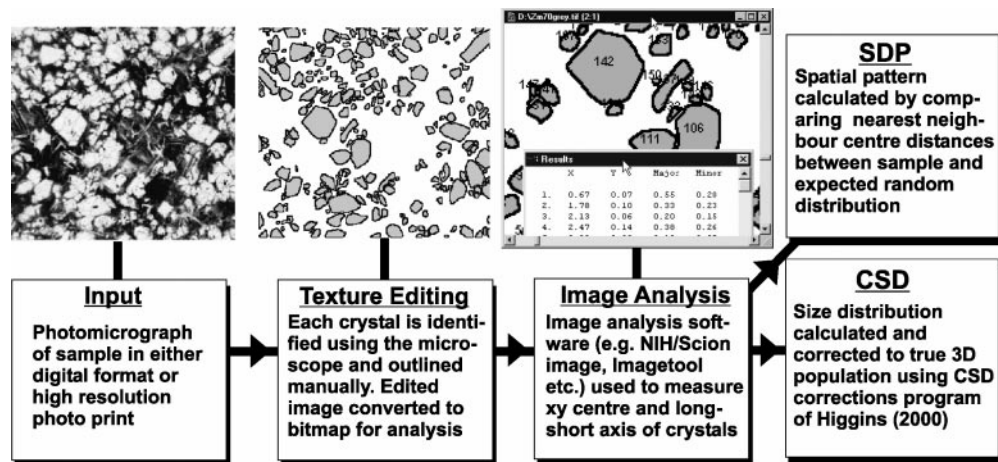


Fig. 2. Flow chart highlighting the technique of textural analysis in this study.

Quantifying the spatial distribution pattern of crystal populations (SDP analysis)

The packing arrangement or spatial distribution pattern (SDP) of crystals provides important information on how a texture is formed (Kretz, 1969; Jerram *et al.*, 1996; Jerram & Cheadle, 2000; Mock *et al.*, 2003). Indeed, the packing arrangement required to form a touching framework is dependent on how the crystals are clustered. For example, small crystal modal abundances can result in a touching framework if the crystals are highly clustered and thus form ‘chains’ of connected crystals (e.g. Fig. 1c).

A method to quantify the SDP of grains and crystals in thin section was introduced by Jerram *et al.* (1996). This technique is based on the ratio between the mean nearest neighbour distance (NND) of objects in the sample and the mean NND expected for a random distribution of points with the same population density as the sample. The mean NND for the sample, r_A , is defined as

$$r_A = \frac{\sum r}{N} \quad (1)$$

where r is the NND, and N is the number of individuals measured. The predicted mean NND for a random distribution of points, r_E , is defined as

$$r_E = \frac{1}{2\sqrt{\rho}} \quad (2)$$

where ρ is the density of the observed distribution. The ratio of the observed and the predicted nearest neighbour distances can then be described by

$$R = \frac{r_A}{r_E} \quad (3)$$

or

$$R = \frac{2\sqrt{\rho} \sum r}{N} \quad (4)$$

where R is a quantification of the SDP.

Finally, to compare how the SDP (R value) varies with different reference textures, a plot of R value vs porosity (% matrix) is used (Jerram *et al.*, 1996). Figure 3 shows the R value vs porosity (% matrix) plot with some reference textures plotted [adapted from Jerram (1996) and Jerram *et al.* (1996)]. The reference textures have known three-dimensional (3D) spatial patterns (Fig. 3a–d), and have been sectioned to generate 2D textures, which can be measured for R value and porosity. These textures then provide reference points on the R value vs porosity (% matrix) plot, which can be used to interpret real rock textures. The line marked RSDL is the Random Sphere Distribution Line, and represents the SDP of randomly packed spheres of differing modal abundance. The random close-packed texture (Fig. 3c) marks the low-porosity termination of this line, because it is the closest possible natural packing of randomly packed, equal-sized spheres (see Jerram *et al.*, 1996). The dotted horizontal line represents the boundary between an ordered and a clustered distribution of spheres and corresponds to the random close-packed sphere texture, reducing porosity by crystallization on the spheres. Hence the R value remains constant as porosity decreases. Samples plotting above the RSDL have a mean NND larger than expected in comparison with randomly packed spheres, which is achieved by having a more ordered distribution resulting in a higher mean NND. Conversely, textures that plot below the RSDL have a mean NND that is lower than expected for random packing and is achieved by more clustered textures where individuals are closer together, thus reducing the sample mean NND with respect to random mean NND. Thus the porosity (% matrix) vs R plot provides a means to compare 2D SDP analyses from rock textures with 2D SDP analyses from sections through known 3D reference textures (Jerram *et al.*,

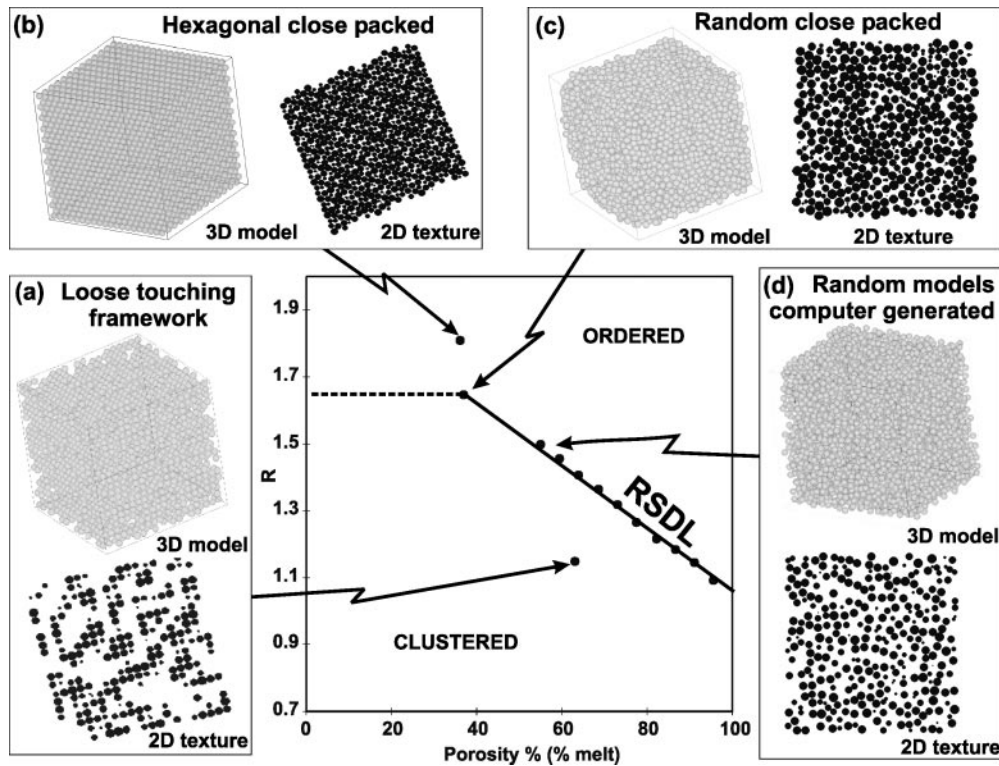


Fig. 3. Porosity (% melt) vs R plot showing position of certain reference textures. RSDL, Random Sphere Distribution Line. (a) Loose-packed touching framework of spheres, (b) hexagonal close packed, (c) random close packed (Finney, 1970), and (d) computer-generated, random models of different porosity. R values are calculated from 2D sections through known 3D textures, providing a method for comparing 2D rock textures with known 3D reference models [adapted from Jerram (1996) and Jerram *et al.* (1996)].

1996). Jerram *et al.* (1996) also modelled how the R value would vary with changing porosity as a result of mechanical compaction, overgrowth and with grain-size variation or sorting (see insert in Fig. 5).

In this study, the positions of the centres of the phenocrysts, as determined by image analysis (e.g. Fig. 2), were used to calculate an R value [equation (4)] as a measure of the SDP of the 2D thin section. Image analysis was also used to determine the matrix proportion of each sample.

Quantifying the size distribution of crystal populations (CSD analysis)

The population of crystal sizes in an igneous rock, as defined by their CSD, contains important information about crystal growth, nucleation and residence histories in the magma system (Marsh, 1998). In the case of a log–linear CSD in a steady-state open system, the population density of the crystals (n) is expressed as

$$n = n_0 \exp \left[\left(-\frac{L}{G\tau} \right) \right] \quad (5)$$

where L is crystal size, G growth rate, τ residence time, and n_0 nucleation density. Linear regression analysis of the CSD curve—a plot of crystal size (L) vs

logarithmic population density of that size [$\ln(n)$]—provides a measure of growth rate/residence time (slope) and nucleation density (intercept) (Marsh, 1998). Deviations of the CSD from straight ‘simple’ patterns can reflect different processes during the crystallization of magma batches, e.g. mixing of crystal populations or Ostwald ripening, etc. (Marsh, 1998; Higgins, 1999; Zieg & Marsh, 2002). In this study, the size distributions of the long axes of crystals, as measured with image analysis software (e.g. Fig. 2), were corrected for 2D–3D effects using the method and software of Higgins (2000): CSD Corrections version 1.2.

Using the textural analysis techniques described above, combined with additional petrographic information, we will now examine examples of naturally occurring clustered crystal populations.

CLUSTERED CRYSTAL POPULATIONS

Crystal clusters (also known as clots, clumps or glomerocrysts) are common if not almost ubiquitous in phenocryst populations. Lavas containing

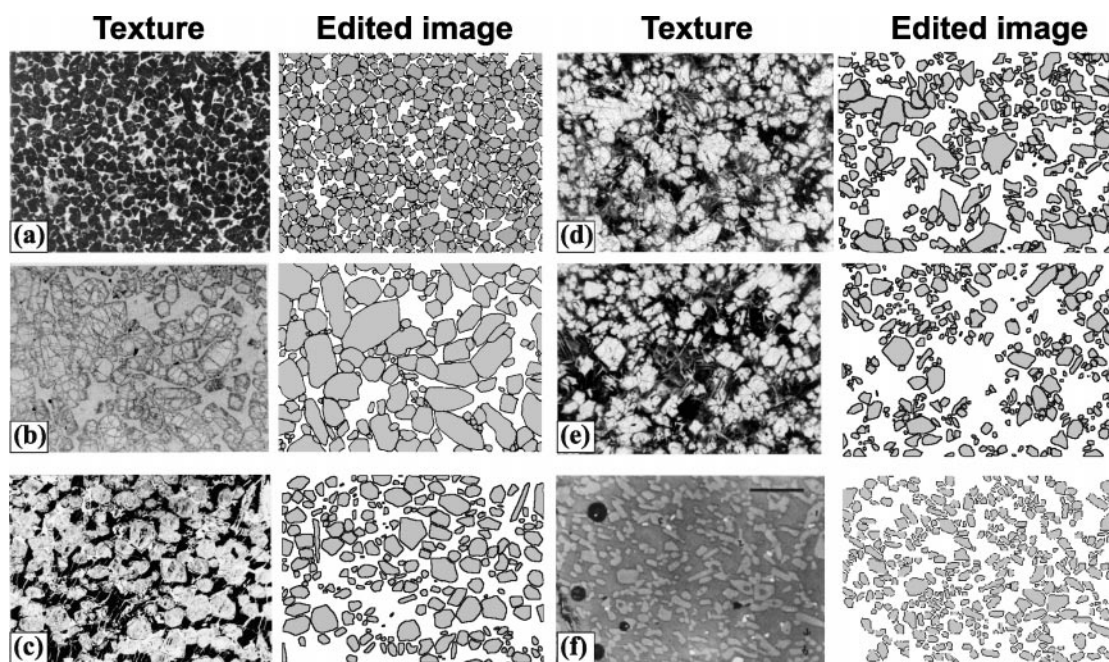


Fig. 4. Original textures and digital edited images from olivine cumulates. (a) Alexo komatiite flow, Abitibi greenstone belt, Canada [sample from N. T. Arndt (personal communication, 1995); photo length 14 mm]. (b) Komatiite flow from Victoria area, Kambalda, western Australia [sample from C. M. Leshner (personal communication, 1995); photo length 16 mm]. (c) Vammala komatiite, western Finland (photo length 11 mm). (d) and (e) B2 zone from Joe's Flow komatiite, Belingwe greenstone belt, Zimbabwe. (f) Olivine cumulate sample from the Campbell *et al.* (1978) centrifuge experiment (photo length 0.5 mm).

glomeroporphyritic crystal populations can have compositions ranging from basalt to dacite (Garcia & Jacobson, 1979; Schwindinger & Anderson, 1989; Halsor & Rose, 1991; Jerram *et al.*, 1996). Garcia & Jacobson (1979) reported the presence of crystal clots of olivine, plagioclase, pyroxene, amphibole, and magnetite within the calc-alkaline magmatic rocks of the High Cascade Range, USA. They used a combination of textural and geochemical evidence to show that the origin of the clots was magmatic and not the product of breakdown reactions between amphibole and melt as previously thought. Schwindinger & Anderson (1989) reported that olivine phenocrysts from the 1959 Kilauea Iki eruption typically formed glomeroporphyritic aggregates of 2–16 crystals. Murata & Richter (1966) had previously suggested that these formed by entrainment of crystal aggregates from a pre-existing cumulate. The actual clumping mechanism invoked by Schwindinger & Anderson (1989) is that of synneusis (the swimming together of crystals), which would most probably occur in a melt-rich environment in which crystals settled and impinged on each other.

In the section below we examine known touching frameworks of crystals (both olivine and plagioclase examples) that have formed in lava flows, and whose textures are quenched at an early enough stage to limit post-framework (post-cumulus) processes from moderating the primary framework (cumulate) texture.

Olivine crystal frameworks

One set of rock textures that we are confident form a 3D touching crystal framework and that show a wide range of modal crystal contents are komatiite cumulates. These cumulates formed from olivine phenocryst accumulation in low-viscosity (~ 1 Pa s) highly magnesian komatiitic melts (> 18 wt % MgO). The olivine crystals would have had relatively high settling velocities ($\sim 10^{-5}$ m/s) and thus only the chills would have frozen quickly enough to trap an unsupported population of olivine crystals. The cumulate zone at the base of a komatiite lava flow is known as the 'B' zone in komatiite classification and referred to specifically as the 'B2' zone for polyhedral olivine crystals (Pyke *et al.*, 1973; Arndt *et al.*, 1977). Samples were studied from four komatiite flows: the Alexo flow, Abitibi greenstone belt, Canada; Kambalda, Western Australia; Vammala, western Finland; Joe's Flow, Belingwe greenstone belt, Zimbabwe (Fig. 4). [For more information on the Alexo komatiites see Arndt (1986); for Belingwe, see Nisbet *et al.* (1987) and Renner *et al.* (1994); for Kambalda, see Leshner & Arndt, (1995).]

Spatial distribution pattern (SDP)

The SDPs of all of the natural olivine crystal frameworks measured in the study are presented on the porosity (% matrix) vs R plot in Fig. 5, along with

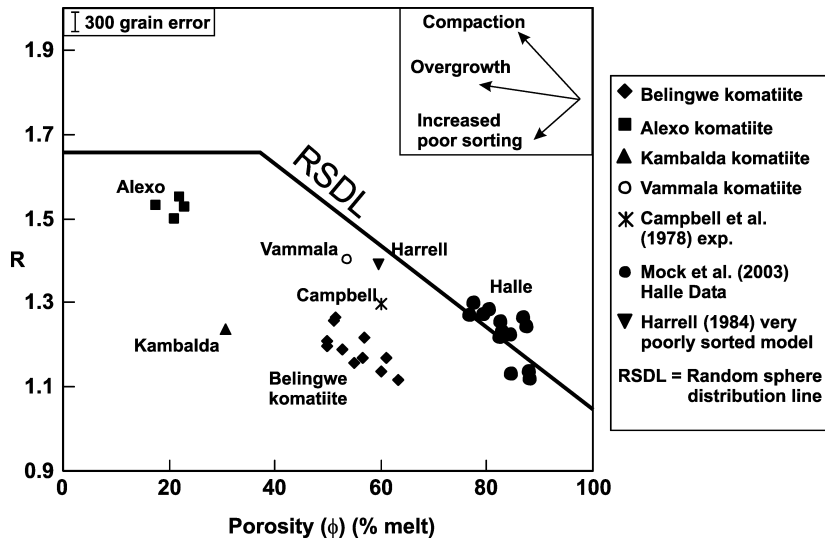


Fig. 5. Porosity (% melt) vs R value for examples of olivine crystal frameworks. Included are data points for randomly distributed crystal populations from Mock *et al.* (2003) and a very poorly sorted model from Harrell (1984). Three vectors highlighting the variation of R value with compaction, overgrowth and increased poor sorting are given from Jerram *et al.* (1996).

the results for Harrell's (1984) reference sample for a very poorly sorted texture and for randomly packed phenocrysts from the Halle igneous complex, Germany (from Mock *et al.*, 2003). The olivine samples show a wide diversity in their SDPs, but all plot below the RSDL, suggesting that many of the examples are composed of clustered crystal frameworks. However, it is important to be certain that their departure from the RSDL is not just a function of variation in the grain-size distribution or sorting of the samples. The standard grain-size sorting scale is the inclusive graphic standard deviation (σ_I) (Folk, 1968). This is calculated by measuring the grain size in phi units ($-\log_2$ diameter) at points along a cumulative frequency plot of grain-size variation. The classification scheme is: very well sorted ($\sigma_I = 0-0.35$); well sorted ($\sigma_I = 0.35-0.5$); moderately well sorted ($\sigma_I = 0.5-7.0$); moderately sorted ($\sigma_I = 0.7-1.0$); poorly sorted ($\sigma_I = 1.0-2.0$).

Jerram *et al.* (1996) originally modelled the effect of grain-size sorting on R values and suggested that increased poor sorting causes samples to plot below the RSDL according to the vector shown in Fig. 5. The effect of crystal sorting in igneous rocks on their location on the porosity vs R plot can be quantified by comparing the location of the known, very poorly sorted reference sample (from Harrell, 1984) with the location of the unsorted samples which would lie on the RSDL. Also, randomly distributed natural populations are given by the Mock *et al.* (2003) data. The very poorly sorted reference sample and the natural random samples plot close to the RSDL, implying that grain-size sorting variations cannot alone account for the relatively large deviations of the olivine samples

from the RSDL. The grain-size distributions in the komatiite samples studied here are moderately well sorted to moderately sorted: Belingwe $0.79-1.04\sigma_I$; Vammala $0.62\sigma_I$; Kambalda $0.85\sigma_I$; Alexo $0.49-0.68\sigma_I$. From this we conclude that the effect of grain-size sorting on the R value in populations of crystals grown from a melt is very small and thus the porosity vs R plot shows that the komatiites have clustered crystal populations; however, further work would be required to fully model these effects on realistic crystal populations.

The Alexo samples plot below the RSDL, and consist of a very well-packed distribution of moderately well-sorted olivine crystals. The Vammala example plots closer to the RSDL, and appears to consist of a loosely packed touching framework that is slightly less clustered than the Alexo samples. The Belingwe and Kambalda komatiites plot much further away from the RSDL and are thus interpreted to consist of very clustered crystal frameworks. Subtle variations in crystal sorting between samples may account for some of the scatter in the Belingwe samples (Fig. 5). The Belingwe examples themselves define a packing variation (mechanical compaction) trend, with an increase in R value being accompanied by a decrease in porosity. The Kambalda sample plots on an overgrowth trend from the Belingwe samples. The sorting characteristics for both examples are similar, and we suggest it is possible to produce the SDP for the Kambalda komatiite from the overgrowth of an original distribution like that of the Belingwe examples.

The data from the Belingwe komatiite warrant further discussion because they provide an excellent

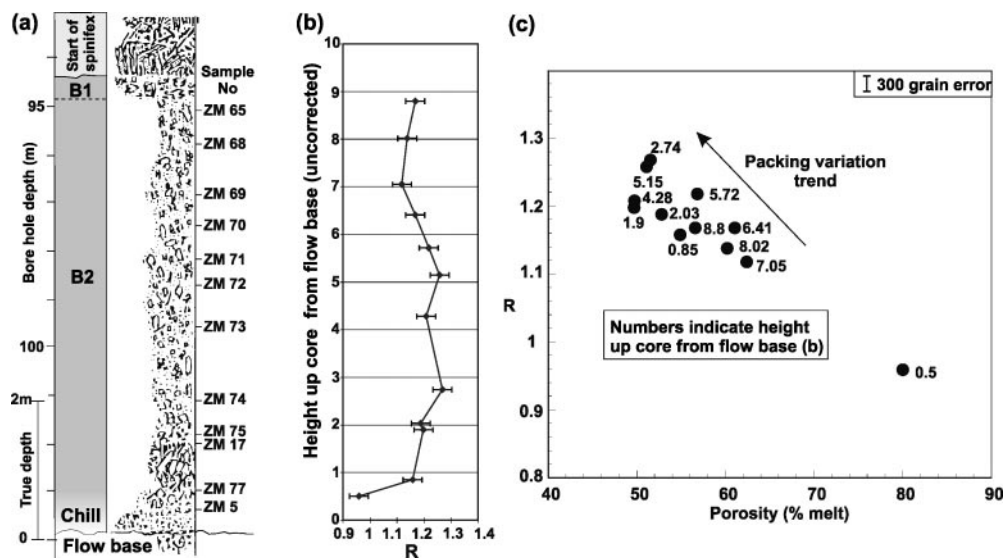


Fig. 6. (a) Sample locality, (b) height up cumulate zone and (c) R value variation as a function of porosity, for Joe's Flow komatiite, Belingwe greenstone belt, Zimbabwe.

example of the potential use of the porosity vs R value plot. The samples are all taken from the same B2 cumulate horizon from Joe's Flow. Figure 6 shows the location of the samples in the cumulate zone with a porosity vs R plot indicating the height of each sample in the cumulate zone. With the exception of the samples near the very base of the cumulate zone, the samples in the central and lower parts show higher R values with lower porosities and the samples toward the upper part of the flow have lower R values and higher porosity. What this clearly highlights is that crystals in the upper parts of the cumulate zone are more loosely packed than those lower in the zone. The range of packing shown by these samples can be explained in terms of the competition between the rate of accumulation of the crystal mush and the rate of advance of the freezing floor of the komatiite (Renner, 1989). The lowermost (below 2 m) samples have low R values, because the rapidly advancing freezing front at the base of the flow would have trapped and frozen-in the accumulating crystals, thereby preventing compaction caused by the weight of the overlying crystal framework. The samples from the rest of the cumulate zone (above 2 m) formed in the region of the flow where crystal accumulation outpaced the freezing front at the base of the flow and hence were able to compact before being frozen-in. The data therefore show a packing variation trend consistent with that of a mechanical compaction trend (Fig. 5).

Additional data to constrain the region of clustered touching frameworks on the R vs porosity plot are gained from experimentally generated, high-porosity,

examples of touching 3D frameworks. A touching framework of olivine crystals, with a melt porosity of ~60%, was produced in a centrifuge experiment carried out by Campbell *et al.* (1978). The occurrence of a touching framework in this sample is unequivocal, because it was accumulated in a centrifuge. This therefore provides another important data point of a known touching framework (Fig. 5).

In summary, the porosity (% melt) vs R plots for the olivine crystal frameworks used in this study show that olivine frameworks display a variety of packing arrangements in three dimensions as indicated by their 2D SDP variation. Such packing variations are important because they reflect the distribution of porosity, in this case frozen melt-matrix, within the sample. This may be of paramount importance in examples such as Vammala, where the nickel sulphide is trapped in the frozen intergranular space, as with other komatiite-hosted nickel sulphide deposits (Naldrett & Campbell, 1982).

Where do the olivine crystal clusters come from?

It is clear that the cumulate B2 zone of Joe's Flow komatiite is made from a population of glomeroporphyritic olivine phenocrysts. The trapped phenocrysts in the basal chill (e.g. ZM5, Figs 6 and 7a) of Joe's Flow give a representative sample of the phenocryst population before further olivine accumulation within the flow, and will closely resemble the phenocryst population that the lava flow contained during emplacement (Fig. 7a). Olivine glomerocrysts are known

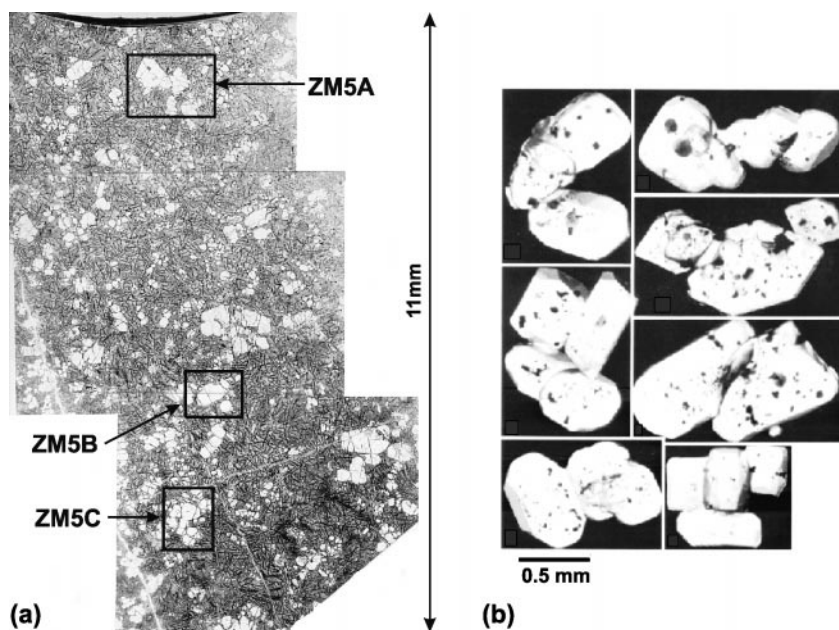


Fig. 7. (a) Photomontage of thin-section sample ZM5 from the basal chill of Joe's Flow komatiite. The glomerocrysts chosen for geochemical analysis are highlighted (ZM5A, ZM5B and ZM5C). (b) Olivine clumps from Kilauea Iki, Hawaii. Clumps are dissolved out from lapilli and mounted in resin [reproduced from Schwindinger & Anderson (1989)].

from modern eruptions such as that of Kilauea Iki (e.g. Schwindinger & Anderson, 1989) (Fig. 7b) and show a remarkable likeness to those preserved in the chill of Joe's Flow. In olivine-rich magmas, such as komatiites, a variety of different olivine morphologies are possible (Donaldson, 1982), yet in both these examples polyhedral olivines have clustered together. These observations raise the question of how and why do the olivine crystals clump. This question has important implications for where the olivine crystals preserved in the komatiite cumulate zone initially formed, and for the interpretation of textural variation in olivine cumulates in general.

Textural equilibration

The existence of olivine clusters or clumps in the chill of the flow implies that the clumps formed before emplacement of the flow. One possibility is that the clumps formed at depth in a magma chamber long before eruption of the lava flow. Another possibility is that they formed during ascent and eruption of the lava flow. In the clumps from the cumulate zone of Joe's Flow a number of triple junctions between olivine crystals can be found. If these clumps formed in a pre-existing cumulate mush in a magma chamber and were ripped up and incorporated into the komatiite lava flow it is possible that the triple junctions would be equilibrated. Rates of textural equilibration are known only imprecisely (Holness & Siklos, 2000), but Cheadle (1989) estimated that 1 mm diameter olivine grains in

a melt would take approximately 10 years to equilibrate texturally. If the olivine crystals in Joe's Flow became clustered or clumped during the transport of the komatiite through and onto the Earth's surface, they would have had little chance to equilibrate texturally, because the komatiite magma is likely to have taken significantly less than 10 years to be transported from the melt generation zone to the final emplacement location. Examples of olivine triple junctions were identified throughout the cumulate zone, and dihedral angles were measured (Fig. 8a). Figure 8b shows the cumulative frequency of dihedral angles from this study plotted against the equilibrium curve (Harker & Parker, 1945) and the unequilibrated curve (Elliott *et al.*, 1997). The unequilibrated curve is calculated by measuring triple junctions on sections through a computer-grown 3D texture of randomly oriented grains (Elliott *et al.*, 1997). In this study 48 triple junctions were measured, providing 144 angles. The curve for Joe's Flow (Fig. 8b) lies between the two curves with parts of the data following the unequilibrated curve. The safe conclusion that can be derived from this plot is that the clumps within Joe's Flow are not fully texturally equilibrated.

Glomerocryst composition

The rationale for studying the composition of the glomerocrysts within the chill is to constrain the timing of the crystal clustering or clumping process. We

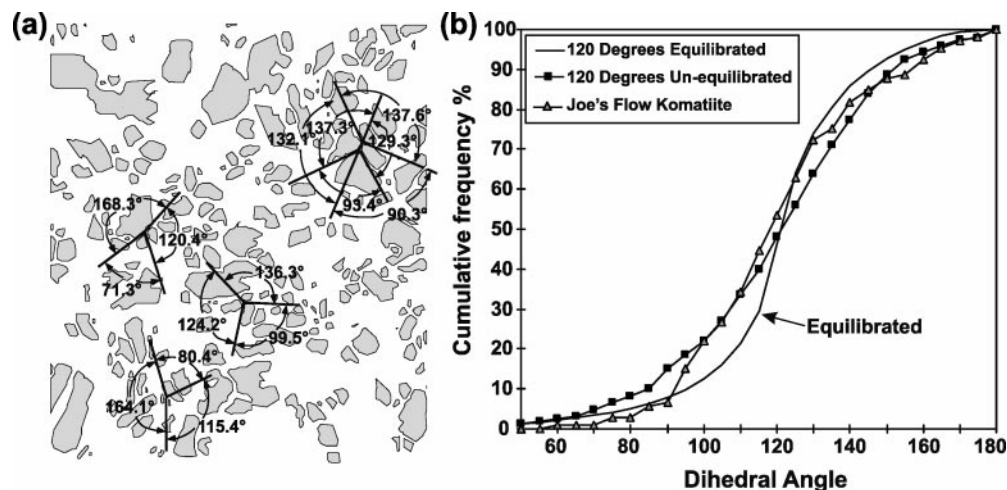


Fig. 8. Dihedral angles from Joe's Flow komatiite, Belingwe greenstone belt, Zimbabwe. (a) Texture showing measurement of dihedral angles; (b) cumulative frequency curve of measured angles from glomerocrysts within Joe's Flow komatiite compared with that of the 120° equilibrium curve (Harker & Parker, 1945), and the 120° unequilibrated curve (Elliott *et al.*, 1997).

know that the clusters are present in the chill and therefore were present directly before the cumulate zone formed, but did the clusters form during flow or were they entrained from a pre-existing cumulate zone from a magma reservoir with a high-level magma chamber?

Analyses of olivine were obtained at the Department of Earth Sciences, University of Manchester, by electron probe microanalysis (EPMA), using a modified Cambridge Instruments Geoscan EPMA equipped with a Link Analytical 8.60 energy dispersive system (EDS) and ZAF 4 software. The samples used were polished thin sections with a 20 nm carbon film. The operating conditions were 15 kV electron beam accelerating voltage, 75° X-ray take-off angle, 3 nA specimen current on cobalt metal with a count time of 100 liveseconds, and 2.5 KCPS output count rate from cobalt metal with 18% detection system dead time. The beam width was 1 μm . Typical errors for elements in an olivine analysis are ± 0.147 %ELEMENT for magnesium (Mg) and ± 0.150 %ELEMENT for iron (Fe), which result in an error in the forsterite (Fo) calculation of ± 0.22 Fo.

Traverses across polyhedral olivine grains in the cumulate zone of Joe's Flow revealed constant composition cores (Fo_{91.4}) with rims zoning to values as low as Fo₈₈ (Renner *et al.*, 1994). The low-forsterite rims are interpreted to have formed as an overgrowth from the interstitial liquid trapped in the pore space after accumulation. Phenocrysts trapped in the chill would not be expected to have such rims. The zoning patterns can clearly help resolve when the olivine crystals clumped together. If they clumped together after an amount of overgrowth, then the forsterite content at the contact of the crystals would

constrain the timing of clumping. Zoning profiles across glomerocrysts in the basal chill of Joe's Flow are shown in Fig. 9.

Glomerocryst ZM5A was studied in detail to quantify the extent of zoning in the glomerocrysts displaying iron-rich rim values. To complement the profiles (Fig. 9) and to give a good coverage of the whole glomerocryst, extra analysis points were chosen. These extra points are shown in Fig. 10 in a composition–texture map contoured for forsterite content. The large olivine crystal in the glomerocryst is normally zoned with forsterite varying from Fo_{92.1} to \sim Fo₈₈, with one measurement as low as Fo_{86.4}. The forsterite variation around the rim is irregular, ranging from Fo_{91.9} to Fo_{86.4}.

The calculated liquid composition (less phenocrysts) on eruption of Joe's Flow is ~ 20 wt % MgO (Renner *et al.*, 1994). The occurrence of zoned glomerocrysts with rim compositions lower than Fo₉₁ (not in equilibrium with the liquid they are in contact with) may be interpreted in four ways:

(1) they represent entrained, already zoned, phenocrysts, e.g. from a pre-existing cumulate mush. However, in this case we would expect to see some reverse zoning as the rims would be in contact with higher Fo liquid during eruption and transport.

(2) The previously calculated (Renner *et al.*, 1994) liquid composition on eruption of Joe's Flow is in error and should be ~ 15 rather than 20 wt % MgO (Silva *et al.*, 1997). The edge of the glomerocrysts would then be in equilibrium with this lower MgO liquid surrounding the crystals. Again, this is very unlikely, as much evidence exists that the liquid composition on eruption of Joe's Flow was ~ 20 wt % MgO [see arguments of Renner *et al.* (1994)].

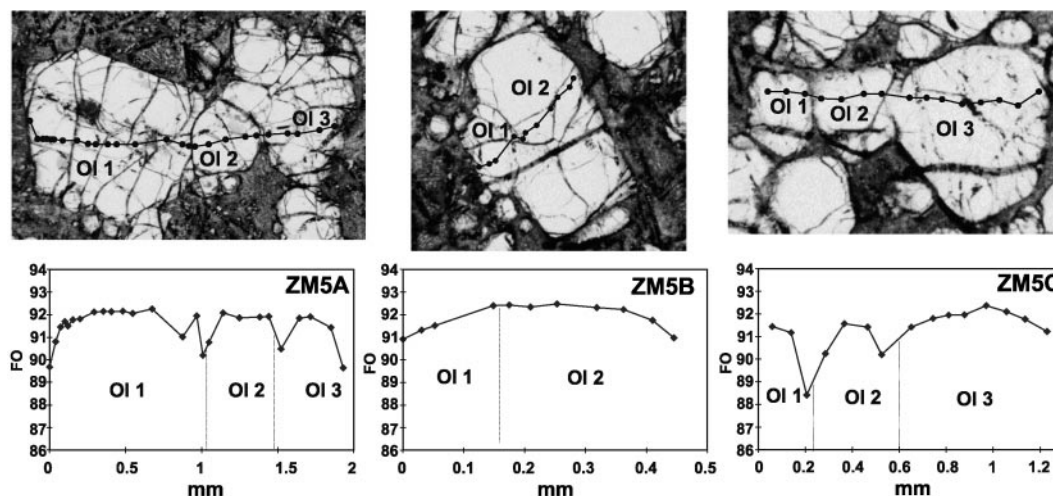


Fig. 9. Forsterite concentration profiles across three glomerocrysts (ZM5A, ZM5B and ZM5C) from the basal chill zone of Joe's Flow komatiite (see Fig. 7 for locations).

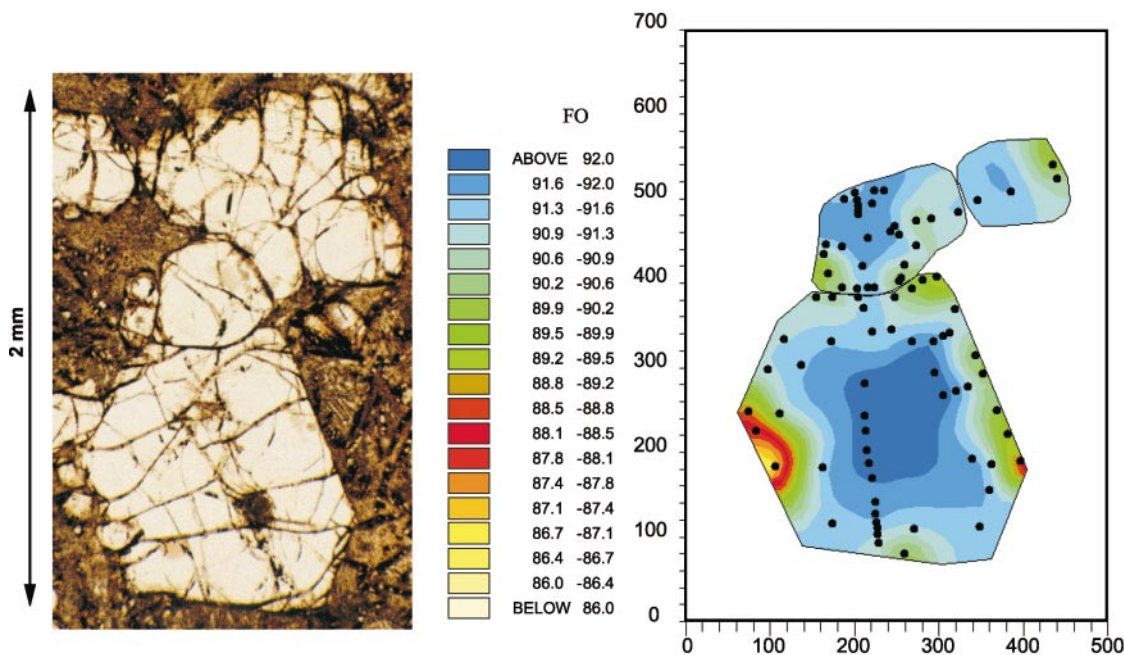


Fig. 10. Forsterite mol % contour map for glomerocryst ZM5A. Zoning within the phenocryst is coloured according to forsterite content. The electron microprobe analysis points are indicated by the black dots. Contouring is done by bi-linear interpolation of the given data points using the UNIMAP software package.

(3) The edges of the glomerocrysts are not in equilibrium with the bulk chilled liquid because cooling and crystal growth was too rapid for the liquid immediately in contact with the crystals to homogenize with more distant melt.

(4) The zoning is a consequence of subsolidus Mg diffusion between the olivines and the matrix.

The independent evidence for the liquid composition being 20 wt % MgO and the variability of the forsterite composition around the rims suggests that explanations (3) and (4) above are most likely. The rim compositions therefore cannot constrain whether the clusters formed before or during the eruption of the flow.

How fast do the olivine crystal frameworks form?

Silva *et al.* (1997) calculated settling rates for individual and clustered crystals in the Belingwe komatiites in the range from 0.05 to 0.1 mm/s, which means that a crystal mush framework would have formed within 3 days in an 11 m thick flow. Therefore, clusters of olivine crystals in komatiite flows would accumulate rapidly (days to tens of days, depending on flow thickness).

Investigation of the CSDs in the Belingwe komatiites can be used further to investigate the changing crystal population from eruption to cumulate framework development. This is possible because the trapped phenocryst population in the basal chill (sample ZM5) provides the CSD of the crystal population before the development of the cumulate zone. An aspect ratio of 1:1:1.5 was used in the CSD correction for the Belingwe samples based on the statistics of the short and long axis measurements (Higgins, 1994). Figure 11 shows the CSD plots for the basal chill sample (ZM5) and for cumulates from the central parts (samples ZM72, 74, 73, 77) of the B2 zone. Samples from the upper part of the cumulate zone were avoided because of the presence of hopper olivine morphologies derived from the upper part of the flow. On first inspection, the CSD plots for the chill are of similar shape to those for the samples from the cumulate zone (Fig. 11a), differing only in population density, as would be expected for the lower modal abundance of the crystals in the former. This supports the interpretation that the B2 zone represents a primary cumulate derived from the transported crystal population carried by the komatiite flow during eruption, as represented in the chill (Renner, 1989). The slight kink at the larger size range is due to a small amount of larger entrained olivine xenocrysts characterized by a higher forsterite content ($Fo_{92-93.6}$) (Renner *et al.*, 1994).

To compare the chill population with the cumulate population we need the two samples to have the same overall volumetric proportions (modal abundance), as the cumulate zone represents an accumulation of the phenocryst population recorded in the chill. This is achieved by adjusting the area occupied by the crystals in the chill so that the recalculated crystal modal abundance is similar to that of the cumulate zone (e.g. 40–50%). When the population density in the chill sample is recalculated in this way (Fig. 11b), the curves completely overlap with the exception of the very small crystal sizes. This may indicate that some of the small crystals in the cumulate zone were resorbed before the population was frozen. Such a kink in the small sizes could therefore represent the onset of textural coarsening (e.g. Higgins, 1998). However, it is also possible that the slight difference in curves is due to

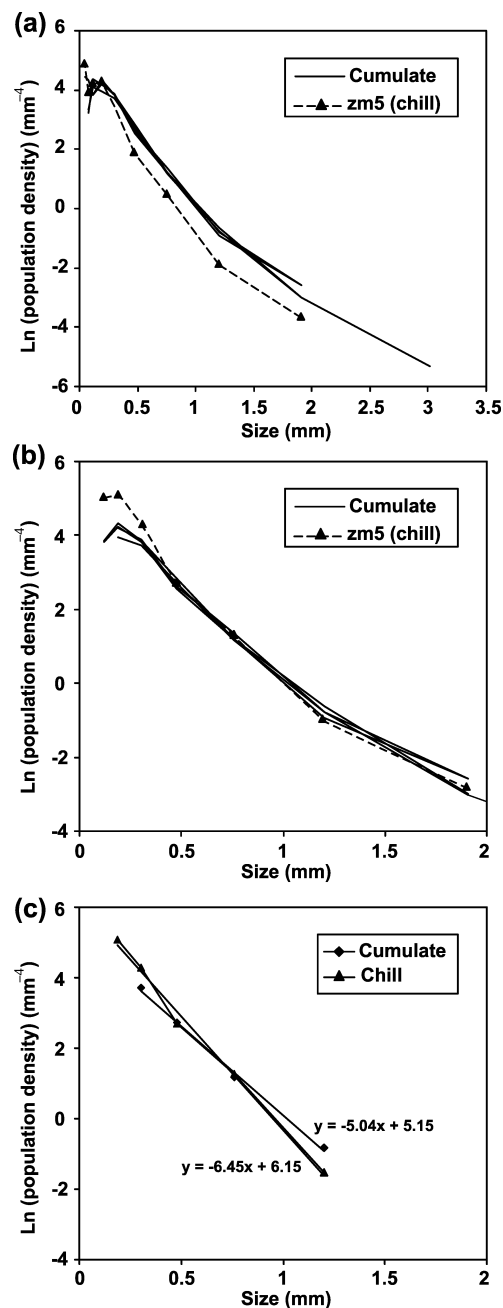


Fig. 11. CSD plots for the Belingwe komatiite cumulate and chill zones. (a) Raw CSD plots; (b) chill recalculated to same population density; (c) CSDs recalculated minus the coarse tail. CSDs corrected using CSD Corrections version 1.2, using a 1:1:1.5 aspect ratio.

errors in the 3D recalculation of the CSD in the small size bins (Higgins, 2000). Higgins (2002) suggested using a plot of characteristic length (CSD slope) vs modal proportion (volumetric phase abundance) to compare CSD plots. We have refrained from using the characteristic length vs modal proportion (volumetric phase abundance) in this study, because the

variation in modal abundance between the samples is due to the accumulation of the crystals from one sample to the other, and not due to changes between two static CSD patterns. Therefore, we compare only the characteristic length (CSD slope).

As stated above, the CSD data in this study have been recalculated from the 2D data to their representative 3D distribution by using the 'CSD Corrections' program of Higgins (2000). We recalculated the 3D CSD from the 2D data with the larger crystal sizes removed to obtain a better estimate of the 3D crystal population without the xenocrystal olivines. Figure 11c shows the CSDs for the chill and a representative cumulate example recalculated minus the coarse tail to account for the larger entrained phenocrysts (and with the kinks at the smallest size bins removed). Renner (1989) has calculated that the flow took approximately 100 days to cool below its solidus, assuming conductive cooling and by comparison with the cooling rates measured in the Hawaiian lava lakes. Consequently, the maximum residence time for growth or enlargement of the crystals in the cumulate zone is about 100 days. The growth rate of the euhedral olivine crystals during the freezing of the flow can be simply calculated by comparing the mean grain size of the phenocrysts in the chill (0.18 mm) with that of the phenocrysts in the cumulate zone (0.23 mm). Using a freezing time of 100 days gives an olivine growth rate of $\sim 6 \times 10^{-9}$ mm/s. This rate compares well with previous studies, which have used estimates of olivine growth rates between 2.4×10^{-8} mm/s (Armienti *et al.*, 1994) and 1×10^{-9} mm/s (Marsh, 1988; Mangan, 1990). We can use this range of growth rates to estimate the growth or residence time of the olivine crystals before they were frozen into the chill. Using the gradient from the curve in Fig. 11c, it can be calculated that the olivines in the chill took between 72 and 1800 days to grow. The population in the chill itself may be composed of crystals that grew during flow across the Earth's surface or in a magma chamber, and may therefore have grown under different conditions, for example with a slower growth rate. It has been suggested that an order of magnitude of growth rate difference occurs in plagioclase systems between magma chamber and lava flow (e.g. Higgins 1996). If we assume a similar scenario for the olivines and use the slowest of the growth rates, then the crystal population frozen in the chill could have been growing in a magma chamber before eruption for up to 1800 days (4.9 years).

Plagioclase crystal frameworks

Clustered crystal frameworks are a common feature of igneous rocks. In the previous section we have

presented a number of examples of olivine textures with a variety of crystal frameworks, many of which were clustered. To address the broader question of the role of clustered frameworks in igneous rock textures, the following section will examine the Holyoke flood basalt, a well-documented basaltic lava flow. In basaltic lava flows, plagioclase is the dominant phenocryst phase, and the objective here is to quantify the properties of plagioclase clusters and hence the building block for the formation of plagioclase cumulate frameworks.

Plagioclase phenocryst and groundmass crystals commonly exhibit prominent clustering, especially in basaltic rocks (e.g. Philpotts & Dickson, 2000; Hoover *et al.*, 2001). The recent reports of touching frameworks of micro-crystals in samples with porosities as high as 75% in melting experiments on the Holyoke flood basalt (Philpotts *et al.*, 1998) provide important constraints on the extent of clustering within magmatic systems at very low crystal contents. Here 1 cm cubes of the Holyoke basalt were melted at different steps of temperature to differing degrees of melt. A hole in the base of the crucible allowed melt to escape during the experiments, thus allowing the identification of touching frameworks at high temperature [see Philpotts & Carroll (1996) and Philpotts *et al.* (1998) for further details of the experiments].

The Mesozoic Holyoke basalt of Connecticut and Massachusetts, like many thick flood-basalt flows, has quench textures (groundmass plagioclase laths with high aspect ratios, strongly zoned subcalcic augite with disequilibrium compositions, skeletal magnetite, and immiscible glasses) throughout its downward-crystallizing roof-crust zone (entablature), and intergranular, recrystallized textures (groundmass plagioclase crystals with lower aspect ratio, equilibrium-composition augite and pigeonite, equant magnetite grains, and interstitial granophyre) in the upward-crystallizing floor zone (colonnade). The quench textures in the entablature are interpreted to result from rapid cooling caused by water flooding the surface of the flow soon after eruption (Long & Wood, 1986; Lyle, 2000). Despite the rapid cooling from above, the boundary between the roof and floor zones (entablature–colonnade boundary) in the Holyoke basalt is well above the centre of the flow, indicating that crystal-rich plumes must have sunk from the roof to the floor of the magma sheet during solidification. Philpotts & Dickson (2000) implied that the descending mush had to consist of at least 33% crystals (21.5% plagioclase and 11.5% augite). The texture in the lower part of the flow can be interpreted as resulting from recrystallization of the material that sank from the roof (Philpotts & Dickson, 2000). Examples of textures from the Holyoke basalt are presented in Fig. 12, and digitized images of the entablature and colonnade

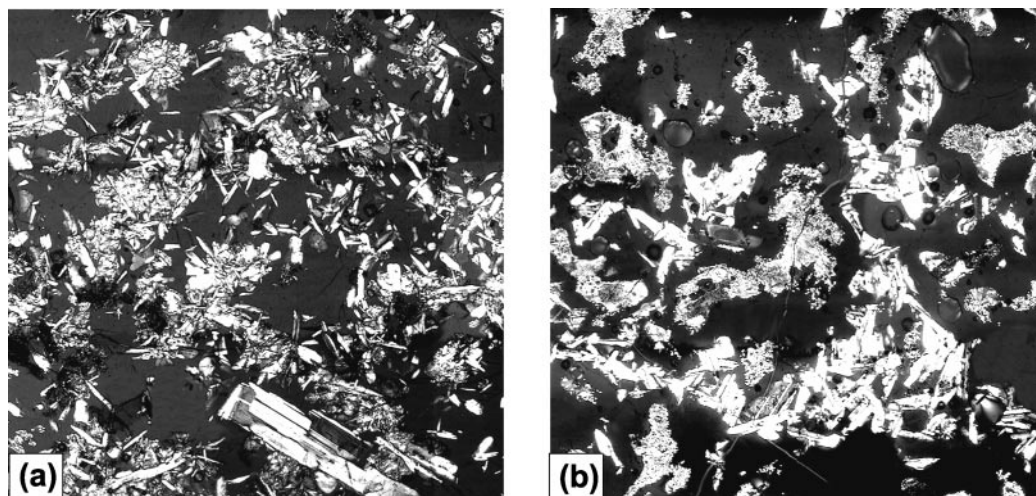


Fig. 12. Partly melted samples from the entablature (a) and colonnade (b) of the Holyoke basalt as seen under partly crossed polars. Sufficient crystals remain to form a touching framework that prevents the block of partly melted rock from changing its shape (Philpotts *et al.*, 1999). Hence the crystals still have their initial positions and only the less refractory ones have been melted and quenched to glass (black). Most plagioclase crystals (white) in the colonnade (b) are clustered into chains that surround the pyroxene grains (granular), whereas in the entablature (a) they occur as radial laths in pyroxene oikocrysts and as separate crystals. Plagioclase phenocrysts are also present in both parts of the flow. Both fields of view are 3.4 mm wide.

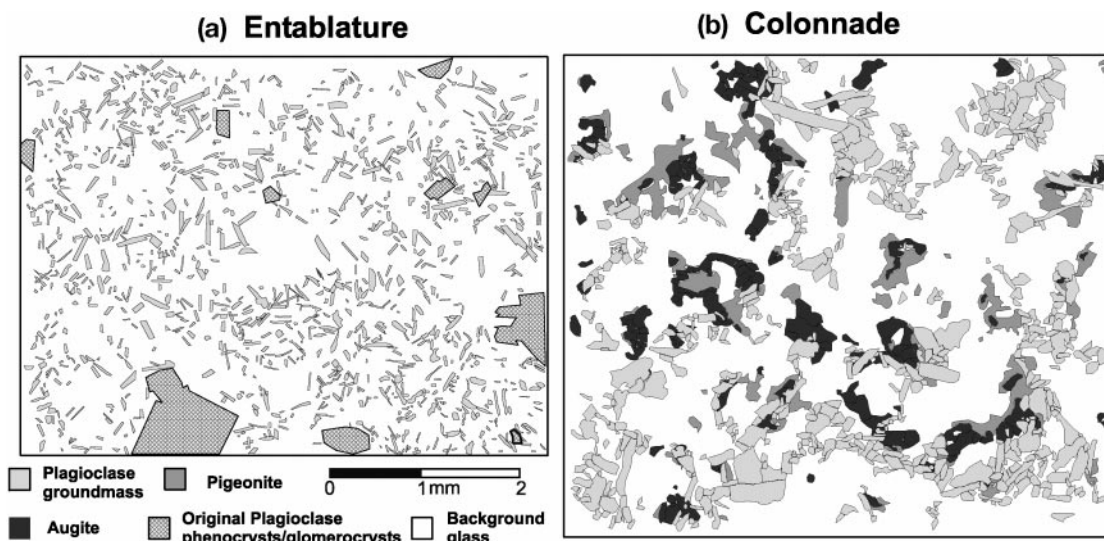


Fig. 13. Examples of digitized plagioclase textures from the entablature (a) and colonnade (b) of the Holyoke basalt.

textures, used to perform CSD and SDP analyses discussed below, are presented in Fig. 13.

In the entablature (Fig. 12a), plagioclase has three modes of occurrence: as phenocrysts ($\sim 5\%$); as high aspect ratio tapering crystals radiating from the centre of rapidly grown subcalcic augite oikocrysts; and as intersertal crystals that are generally tangential to the outer surface of the oikocrysts and that form incipient chains (Philpotts & Dickson, 2000). Although the phenocrysts are commonly clustered, the radial plagioclase

crystals never touch one another (except at the centre of the oikocryst) because they are separated by pyroxene; some of the intersertal crystals touch one another or the tips of the radial plagioclase crystals.

Approximately 60% of the crystal mush in the roof zone is believed to have separated and sunk to the floor of the magma sheet. The texture of the material that sank would have resembled the texture now preserved in the entablature but at an earlier stage of crystallization, as illustrated in the partly melted sample in

Fig. 12a. On sinking to the floor zone of the flow, the pyroxene oikocrysts, which grew initially with disequilibrium compositions, recrystallized to granular aggregates of augite and pigeonite with compositions falling on either side of the pyroxene solvus. This recrystallization took place in the presence of copious residual liquid, which allowed for the nucleation and growth of separate grains. This is in contrast to the subsolidus exsolution of augite and pigeonite, which leads to fine exsolution lamellae in each phase. During recrystallization, most (but not all) of the long radial plagioclase laths recrystallized into shorter crystals, many of which near the margins of the oikocrysts were expelled from the pyroxene patches to join the surrounding intersertal plagioclase crystals. It is at this stage that the clustering of plagioclase crystals is believed to have taken place. With continued slow cooling in the floor zone, euhedral pyroxene crystals grew onto the outside of the granular pyroxene aggregates and the intersertal plagioclase crystals grew to form a 3D network of plagioclase chains (Fig. 12b) surrounding the pyroxene clusters (Philpotts *et al.*, 1999; Philpotts & Dickson, 2000).

How fast do the plagioclase crystal frameworks form?

The Holyoke flow provides an opportunity to determine the approximate time needed to develop a clustered plagioclase framework. CSDs can be employed to estimate the time required to produce the preserved crystal populations found in the entablature and colonnade before the textures were frozen. The plagioclase populations are highlighted in the digitized sections in Fig. 13.

Figure 14 shows CSD plots for plagioclase crystals in the entablature and the colonnade samples from the Holyoke flow (Fig. 13). An aspect ratio of 1:1:3 was used in the CSD correction for the Holyoke samples based on the statistics of the short and long axis measurements (Higgins, 1994). All plagioclase crystals, including the phenocrysts that were present at the time of eruption, are plotted in Fig. 14a (Philpotts & Dickson, 2000). The phenocrysts, however, affect the correction calculation and produce a kinked CSD, because more large crystals are present than would be expected for a single crystallization event. To remove this effect, crystals larger than 0.5 mm (a dimension significantly greater than the groundmass crystals) were removed before applying the 3D correction. This yielded straight CSD plots (Fig. 14b), which can be used to investigate the time required to form the touching crystal framework. Calculations using growth rates of 1×10^{-10} mm/s (Cashman, 1990) give residence times of 57.7 years and 40.5 years, respectively, for the colonnade and entablature crystal populations. If growth rates were slightly higher, say 5×10^{-10} mm/s, because of undercooling resulting from

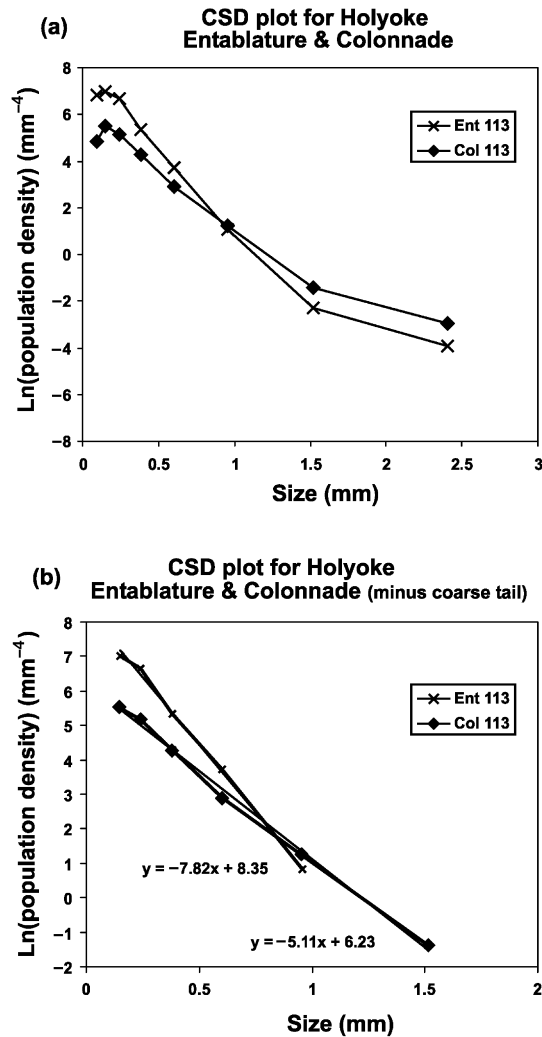


Fig. 14. CSD plots for the Holyoke flood basalt. CSDs corrected using CSD Corrections version 1.2, using a 1:1:3 aspect ratio. (a) Raw CSDs of colonnade and entablature; (b) CSD plots minus coarse tail and kink at very low crystal sizes.

water flooding the surface of the flow, the crystal populations would suggest residence times of 11.5 years and 8.1 years for the colonnade and the entablature, respectively. It has been suggested that the growth rate of plagioclase in magma chambers is of the order of 1×10^{-11} cm/s, and in lavas 1×10^{-10} cm/s (e.g. Higgins 1996). Given that the network forms by the time the magma is only $\sim 30\%$ crystallized, the CSDs point to the framework having formed in less than 17 years for a crystal growth rate of 1×10^{-10} mm/s to less than 3 years for a growth rate of 5×10^{-10} mm/s, when entablature residence times are subtracted from those of the colonnade. These values are consistent with the estimated rate of advance of the downward crystallizing roof zone of ~ 2 cm/day, which would result in the 200 m thick flow solidifying in less than 30 years

(Philpotts *et al.*, 2000). It should be noted that this assumes a uniform cooling rate and the cooling time would be longer if the cooling rate decreased with time.

The resultant textures from the innovative melt experiments on the Holyoke basalt (Philpotts *et al.*, 1998) provide us with important data points, which indicate the variation in spatial packing likely for naturally clustered frameworks. The spatial distribution of the crystals in the entablature is of great importance because the crystals do not form a touching framework (Philpotts *et al.*, 1998). The results of the SDP analysis of the entablature and colonnade, and their significance, will be presented in the context of the other textures considered in this study in the discussion section below.

DISCUSSION

Spatial packing in crystal frameworks

In the present study both touching crystal frameworks and non-touching crystal populations have been investigated. A variety of olivine touching crystal frameworks from komatiites display a marked range of spatial packing arrangements, and a clustered plagioclase crystal framework from the colonnade of the Holyoke flow provides an example of a touching framework at very high porosity. The crystal population in the chill zone of the Belingwe komatiite (Joe's Flow) and the entablature texture from the Holyoke flow provide examples of the spatial packing of non-touching crystal populations. These data points can be used together with existing constraining points (Jerram *et al.*, 1996; Mock *et al.*, 2003) to delineate the regions of touching frameworks and non-touching crystals on an R vs porosity plot (Fig. 15). On this plot, touching frameworks are marked as filled circles and non-touching frameworks are marked as filled triangles. The boundary between the two regions is reasonably well constrained for R values less than 1.3. At higher R values the boundary is less well constrained, because we have found no examples of high-porosity, high R value non-touching frameworks.

Figure 16 shows a summary plot of porosity (% melt) vs R value for the olivine textures of this study, along with the touching and non-touching examples from the Holyoke flow. Additionally, examples of non-touching crystal populations from Mock *et al.* (2003) are included, along with fields for aeolian sands and oolites (Jerram *et al.*, 1996). The aeolian sands and oolites fields provide reference SDPs of well-packed, well-sorted, natural touching frameworks.

One of the major conclusions of this paper is that the crystal frameworks observed in this study and in previous work (Jerram *et al.*, 1996; Mock *et al.*, 2003) allow the definition of distinct fields on the porosity vs R

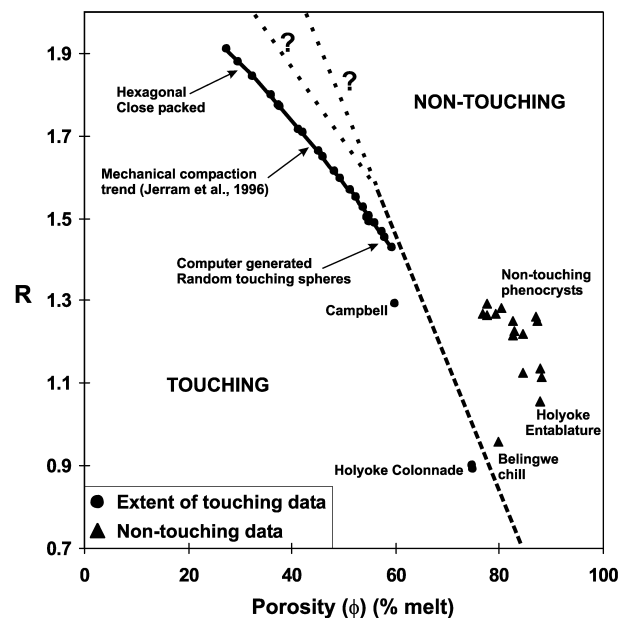


Fig. 15. Porosity vs R value, constraining areas of touching frameworks and non-touching crystals. ●, Touching frameworks; ▲, non-touching crystals.

value plot. These fields define the packing arrangements of (1) non-touching ordered crystals, (2) non-touching clustered crystals, (3) touching clustered frameworks, and (4) touching ordered framework; the RSDL indicates random distributions both touching and non-touching. This plot provides a method of determining whether crystals form a touching framework in three dimensions based on the spatial packing arrangement derived from 2D sections. The measurement of spatial packing in a rock texture can therefore provide important constraints on the texture's origin (e.g. Jerram *et al.*, 1996; Mock *et al.*, 2003; this study) and also may be critical for examining the transition and evolution from non-touching to touching frameworks.

Implications

This study has focused on lava flows with touching crystal frameworks that have been formed and then 'frozen-in' early in their development. Our objective has been to identify the properties of these primary crystal frameworks before significant modification as a result of overgrowth and/or compaction. We have shown that olivine and plagioclase crystal frameworks display a marked variety of spatial packing arrangements. This variety of packing arrangements reflects the variation in the clustering of crystals within the building blocks that form the primary cumulate framework. The variation in the size of, and the clustering

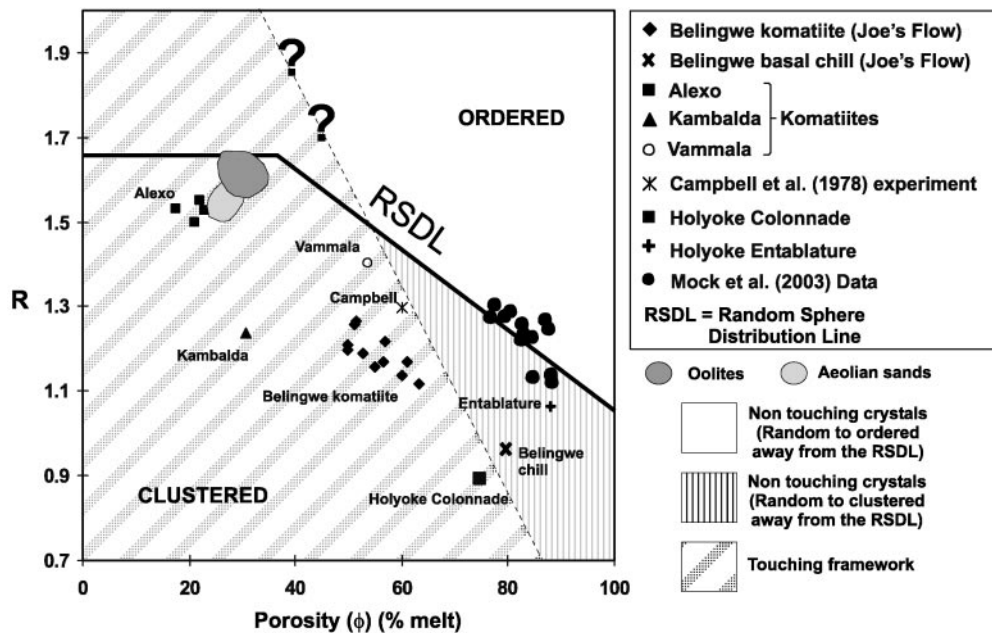


Fig. 16. Porosity (% melt) vs R value for the examples presented in this study. Fields for touching frameworks and non-touching populations are indicated.

within, the building blocks is a function of the processes of nucleation and early crystal growth (Philpotts & Dickson, 2000; Hoover *et al.*, 2001), crystal interaction during settling or movement through liquid (Schwindinger, 1999), and complex recycling histories through the magma plumbing system (e.g. Turner *et al.*, 2003).

Crystal clusters are easily formed in magmas. Crystals may nucleate heterogeneously, and any remobilization of crystals in the magma system or complex settling trajectories caused by different crystal shapes (e.g. Schwindinger, 1999) may lead to crystals touching and forming clusters. Entrainment of plagioclase-rich crystal mush from beneath the Iceland rift, for example, produces a mixed population of phenocrysts in surface flows (Hansen & Grönvold, 2000). This plumbing system is probably relatively simple compared with those in many continental settings. Even at the simplest level of nucleation and crystallization of micro-crystals, it has been shown that complex chaining and crystal networks develop (e.g. Philpotts & Dickson, 2000). Such complex interactions of micro-crystals at very high melt fractions have been invoked to explain the transition from pahoehoe to aa lava characteristics (Hoover *et al.*, 2001).

In the volcanic examples considered here, clustered crystal frameworks form quickly. In more slowly cooled intrusive bodies, clustering would be expected to occur very early in the crystallization history of the magma, although it may occur over longer time-scales because of slower growth rates in the plutonic

environment. Clustering would be enhanced by the reworking of crystal mushes from the walls and roof of the magma chamber, as well as by crystals colliding during settling, and by heterogeneous nucleation. Instabilities in the mush zones at the top of a magma body (Jellinek & Kerr, 2001; Philpotts & Dickson, 2002) could generate crystal-laden plumes, which redistribute individual crystals or clusters of crystals to the floor of the magma chamber, thereby forming the primary high-porosity crystal framework from which a cumulate zone develops. These high-porosity, highly permeable, clustered crystal frameworks permit the easy exchange of melts from the crystal mush to the main magma body, and therefore a large amount of mechanical compaction (from 70% to 35% porosity) of crystal mush could be accommodated before deformation-driven compaction occurs.

ACKNOWLEDGEMENTS

This work has benefited from a University of Durham research grant and a Royal Society travel grant to D.A.J. Part of this work was undertaken when the first author was funded by a National Environmental Research Council (NERC) studentship. C. M. Lesher and N. T. Arndt are thanked for supplying komatiite samples from Kambalda and Alexo. Jenyang Shi and Besim Dragovic are thanked for their help in tracing the plagioclase crystals in the two samples of Holyoke basalt. Kathy Schwindinger and Springer are thanked for permission to reproduce Fig. 7b. This work has

been supported by NSF grants EAR 98-05269 and EAR 99-02890 to A.R.P. Reviews by Michael Higgins, Marion Holness and Michael Zieg, and detailed editorial work by Margorie Wilson were very helpful.

REFERENCES

- Armienti, P., Pareschi, M. T., Innocenti, F. & Pompilio, M. (1994). Effects of magma storage and ascent on the kinetics of crystal growth. *Contributions to Mineralogy and Petrology* **115**, 402–414.
- Arndt, N. T. (1986). Differentiation of komatiite flows. *Journal of Petrology* **27**, 279–301.
- Arndt, N. T., Naldrett, A. & Pyke, D. R. (1977). Komatiitic and iron-rich tholeiitic lavas of Munro Township, northeast Ontario. *Journal of Petrology* **18**, 319–369.
- Boudreau, A. E. & McBirney, A. R. (1997). The Skaergaard layered series: Part III. Non-dynamic layering. *Journal of Petrology* **38**, 1003–1020.
- Bryon, D. N., Atherton, M. P. & Hunter, R. H. (1995). The interpretation of granitic textures from serial thin sectioning, image analysis and three-dimensional reconstruction. *Mineralogical Magazine* **59**, 203–211.
- Burkhard, D. J. M. (2002). Kinetics of crystallization: example of micro-crystallization in basalt lava. *Contributions to Mineralogy and Petrology* **142**(6), 724–737.
- Campbell, I. H., Roeder, P. L. & Dixon, J. M. (1978). Plagioclase buoyancy in basaltic liquids as determined with a centrifuge furnace. *Contributions to Mineralogy and Petrology* **67**, 369–377.
- Carlson, W. D., Denison, C. & Ketcham, R. A. (1999). High-resolution X-ray computed tomography as a tool for visualization and quantitative analysis of igneous textures in three dimensions. *Electronic Geosciences* **4**, 3.
- Cashman, K. V. (1990). Textural constraints on the kinetics of crystallization of igneous rocks. In: Nicholls, J. & Russell, J. K. (eds) *Modern Methods of Igneous Petrology—Understanding Magmatic Processes*. Mineralogical Society of America, *Reviews in Mineralogy* **24**, 259–314.
- Cheadle, M. J. (1989). Properties of texturally equilibrated two-phase aggregates. Ph.D. thesis, University of Cambridge, 140 pp.
- Cooper, M. R. & Hunter, R. H. (1995). Precision serial lapping, imaging and three-dimensional reconstruction of minus-cement and post-cementation intergranular pore-systems in the Penrith Sandstone of north-western England. *Mineralogical Magazine* **59**, 213–220.
- Donaldson, C. H. (1982). Spinifex-textured komatiites: a review of textures, mineral compositions and layering. In: Arndt, N. T. & Nisbet, E. G. (eds) *Komatiites*. London: Allen & Unwin, pp. 213–244.
- Eales, H. V. & Cawthorn, R. G. (1996). The Bushveld Complex. In: Cawthorn, R. G. (ed.) *Layered Intrusions*. Amsterdam: Elsevier, pp. 181–229.
- Elliott, M. T., Cheadle, M. J. & Jerram, D. A. (1997). On the identification of textural equilibrium in rocks using dihedral angle measurements. *Geology* **25**, 355–358.
- Emeleus, C. H., Cheadle, M. J., Hunter, R. H., Upton, B. G. J. & Wadsworth, W. J. (1996). The Rum layered suite. In: Cawthorn, R. G. (ed.) *Layered Intrusions*. Amsterdam: Elsevier, pp. 403–439.
- Finney, J. L. (1970). The geometry of random packing. *Proceedings of the Royal Society of London, Series A* **319**, 479–493.
- Folk, R. L. (1968). *Petrology of Sedimentary Rocks*. Austin, TX: Hemphill, 170 pp.
- Garcia, M. O. & Jacobson, S. S. (1979). Crystal clots, amphibole fractionation and the evolution of calc-alkaline magmas. *Contributions to Mineralogy and Petrology* **69**, 319–327.
- Halsor, S. P. & Rose, W. I. (1991). Mineralogical relations and magma mixing in calc-alkaline andesites from Lake Atatlan, Guatemala. *Mineralogy and Petrology* **45**, 47–67.
- Hansen, H. & Grönvold, K. (2000). Plagioclase ultraphyric basalts in Iceland: the mush of the rift. *Journal of Volcanology and Geothermal Research* **98**, 1–32.
- Harker, D. & Parker, E. R. (1945). Grain shape and grain growth. *Transactions of the American Society of Metallurgy* **34**, 156–195.
- Harrell, J. (1984). A visual comparator for degree of sorting in thin and plane sections. *Journal of Sedimentary Petrology* **54**, 646–650.
- Higgins, M. D. (1994). Numerical modeling of crystal shapes in thin sections; estimation of crystal habit and true size. *American Mineralogist* **79**, 113–119.
- Higgins, M. D. (1996). Crystal size distributions and other quantitative textural measurements in lavas and tuff from Egmont Volcano (Mt. Taranaki), New Zealand. *Bulletin of Volcanology* **58**, 194–204.
- Higgins, M. D. (1998). Origin of anorthosite by textural coarsening: quantitative measurements of a natural sequence of textural development. *Journal of Petrology* **39**, 1307–1323.
- Higgins, M. D. (1999). Origin of megacrysts in granitoids by textural coarsening: a crystal size distribution (CSD) study of microcline in the Cathedral Peak granodiorite, Sierra Nevada, California. In: Fernandez, C. & Castro, A. (eds) *Understanding Granites: Integrating Modern and Classical Techniques*. Geological Society, London, *Special Publications* **158**, 207–219.
- Higgins, M. D. (2000). Measurement of crystal size distributions. *American Mineralogist* **85**(9), 1105–1116.
- Higgins, M. D. (2002). Closure in crystal size distributions (CSD), verification of CSD calculations, and the significance of CSD fans. *American Mineralogist* **87**, 171–175.
- Holness, M. B. & Siklos, S. T. C. (2000). The rates and extent of textural equilibration in high-temperature fluid-bearing systems. *Chemical Geology* **162**, 137–153.
- Hoover, S. R., Cashman, K. V. & Manga, M. (2001). The yield strength of subliquidus basalts—experimental results. *Journal of Volcanology and Geothermal Research* **107**, 1–18.
- Jellinek, M. A. & Kerr, R. C. (2001). Magma dynamics, crystallization, and chemical differentiation of the 1959 Kilauea Iki lava lake, Hawaii, revisited. *Journal of Volcanology and Geothermal Research* **110**, 235–263.
- Jerram, D. A. (1996). The development and application of detailed textural analysis techniques. A case study: the origin of komatiite cumulates. Ph.D thesis, University of Liverpool, 221 pp.
- Jerram, D. A. (2001). Visual comparators for degree of sorting in 2-D and 3-D. *Computers and Geoscience* **27**, 485–492.
- Jerram, D. A. & Cheadle, M. J. (2000). On the cluster analysis of rocks. *American Mineralogist* **84**(1), 47–67.
- Jerram, D. A., Cheadle, M. J., Hunter, R. H. & Elliott, M. T. (1996). The spatial distribution of grains and crystals in rocks. *Contributions to Mineralogy and Petrology* **125**(1), 60–74.
- Kretz, R. (1969). On the spatial distribution of crystals in rocks. *Lithos* **2**, 39–66.
- Leshner, C. M. & Arndt, N. T. (1995). REE and Nd isotope geochemistry, petrogenesis and volcanic evolution of contaminated komatiites at Kambalda, Western Australia. *Lithos* **34**(1–3), 127–157.
- Long, P. E. & Wood, B. J. (1986). Structures, textures, and cooling histories of Columbia River basalt flows. *Geological Society of America Bulletin* **97**, 1144–1155.

- Lyle, P. (2000). The eruption environment of multi-tiered columnar basalt lava flows. *Journal of the Geological Society, London* **157**, 715–722.
- Mangan, M. T. (1990). Crystal size distribution systematics and the determination of magma storage times: the 1959 eruption of Kilauea Volcano, Hawaii. *Journal of Volcanology and Geothermal Research* **44**, 295–302.
- Marsh, B. D. (1988). Crystal capture, sorting and retention in convecting magma. *Geological Society of America Bulletin* **100**, 1720–1737.
- Marsh, B. D. (1996). Solidification fronts and magmatic evolution. *Mineralogical Magazine* **60**, 5–40.
- Marsh, B. D. (1998). On the interpretation of crystal size distributions in magmatic systems. *Journal of Petrology* **39**, 553–599.
- Marsh, B. D. (2002). On bimodal differentiation by solidification front instability in basaltic magmas, part 1: basic mechanics. *Geochimica et Cosmochimica Acta* **66**(12), 2211–2229.
- Mock, A., Jerram, D. A. & Breikreuz, C. (2003). Using quantitative textural analysis to understand the emplacement of shallow-level rhyolitic laccoliths—a case study from the Halle Volcanic Complex, Germany. *Journal of Petrology* **44**, 833–849.
- Murata, K. J. & Richter, D. H. (1966). The settling of olivine in Kilauean magma as shown by lavas of the 1959 eruption. *American Journal of Science* **264**, 194–203.
- Naldrett, A. J. & Campbell, I. H. (1982). Physical and chemical constraints on genetic models for komatiite-related Ni-sulphide deposits. In: Arndt, N. T. & Nisbet, E. G. (eds) *Komatiites*. London: Allen & Unwin, pp. 423–434.
- Nisbet, E. G., Arndt, N. T., Bickle, M. J., Cameron, W. E., Chauvel, C., Cheadle, M. J., Hegner, E., Kyser, T. K., Martin, A., Renner, R. & Roedder, E. (1987). Uniquely fresh 2.7 Ga komatiites from the Belingwe greenstone belt, Zimbabwe. *Geology* **15**, 1147–1150.
- Philpotts, A. R. & Carroll, M. (1996). Physical properties of partly melted tholeiitic basalt. *Geology* **24**(11), 1029–1032.
- Philpotts, A. R. & Dickson, L. D. (2000). The formation of plagioclase chains during convective transfer in basaltic magma. *Nature* **406**(6791), 59–61.
- Philpotts, A. R. & Dickson, L. D. (2002). Millimeter-scale modal layering and the nature of the upper solidification zone in thick flood-basalt flows and other sheets of magma. *Journal of Structural Geology* **24**(6–7), 1171–1177.
- Philpotts, A. R., Shi, J. & Brustman, C. (1998). Role of plagioclase crystal chains in the differentiation of partly crystallized basaltic magma. *Nature* **395**(6700), 343–346.
- Philpotts, A. R., Brustman, C., Shi, J., Carlson, W. D. & Denison, C. (1999). Plagioclase-chain networks in slowly cooled basaltic magma. *American Mineralogist* **84**, 1819–1829.
- Philpotts, A. R., Dickson, L. D. & Gray, N. H. (2000). Role of convection in the solidification of the simplest magma body—a thick flood-basalt flow. *Mineralogical Association of Canada, GeoCanada 2000, Abstracts*, Calgary.
- Pyke, D. R., Naldrett, A. J. & Eckstrand, O. R. (1973). Archean ultramafic flows in Munro Township, Ontario. *Geological Society of America Bulletin* **84**, 955–978.
- Renner, R. (1989). Cooling and crystallisation of komatiite flows from Zimbabwe. Ph.D. thesis, University of Cambridge, 162 pp.
- Renner, R., Nisbet, E. G., Cheadle, M. J., Arndt, N. T., Bickle, M. J. & Cameron, W. E. (1994). Komatiite flows from the Reliance Formation, Belingwe Belt, Zimbabwe I: Petrography and mineralogy. *Journal of Petrology* **35**, 361–400.
- Schwindinger, K. R. (1999). Particle dynamics and aggregation of crystals in a magma chamber with application to Kilauea Iki olivines. *Journal of Volcanology and Geothermal Research* **88**, 209–238.
- Schwindinger, K. R. & Anderson, A. T., Jr (1989). Synneusis of Kilauea Iki olivines. *Contributions to Mineralogy and Petrology* **103**, 187–198.
- Silva, K. E., Cheadle, M. J. & Nisbet, E. G. (1997). The origin of BI zones in komatiite flows. *Journal of Petrology* **38**, 1565–1584.
- Turner, S., George, R., Jerram, D. A., Carpenter, N. & Hawkesworth, C. (2003). Some case studies of plagioclase growth and residence times in island arc lavas from the Lesser Antilles and Tonga, and a model to reconcile apparently disparate age information. *Earth and Planetary Science Letters* (in press).
- Zieg, M. J. & Marsh, B. D. (2002). Crystal size distribution and scaling laws in the quantification of igneous textures. *Journal of Petrology* **43**, 85–101.